

FIG. 2. Fused  $\text{KNO}_3$  switching time,  $t_s$ , and  $1/t_s$  versus applied field at room temperature (copper substrate; sheet copper 2nd electrode).

that the ferroelectric dipoles switch faster at higher temperatures. Linearity at high fields is evident, similar to that of  $\text{BaTiO}_3$  single crystals.<sup>2</sup> Figure 1 also indicates that a decrease in temperature is accompanied by an increase in coercive field. At 30 kV/cm and 20°C this sample yielded a switching time of 15  $\mu\text{sec}$ , in contrast to the results, shown in Fig. 2, where a small copper disk of area  $13.85 \times 10^{-2} \text{ cm}^2$  was used as the second electrode, the sample thickness is approximately the same as that of the sample using silver paint. For this sample a field of 30 kV/cm resulted in a

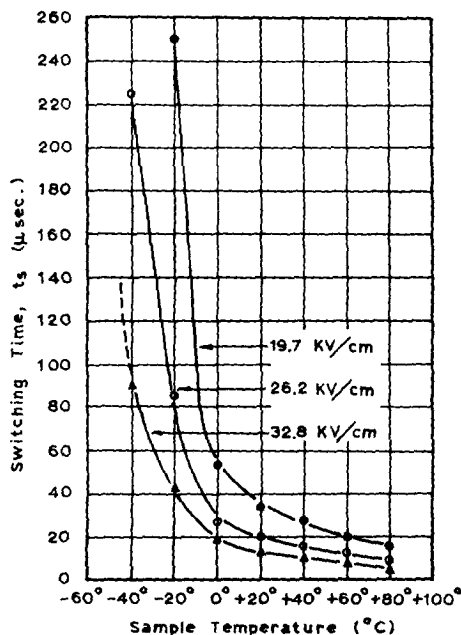


FIG. 3. Fused  $\text{KNO}_3$  switching time versus sample temperature at three different pulsing fields (copper substrate; silver paint 2nd electrode).

switching time of 6  $\mu\text{sec}$ . It is speculated that this difference may have been due to domain deterioration caused by the curing of the silver paint.

Figure 3 illustrates the variation in switching time as a function of temperature for three different pulsing fields. The curves are characterized by a rapid change in switching time at low temperatures followed by a leveling off at higher temperatures.

The peak switching current density versus applied field is shown in Fig. 4 with temperature as a parameter. Again linearity

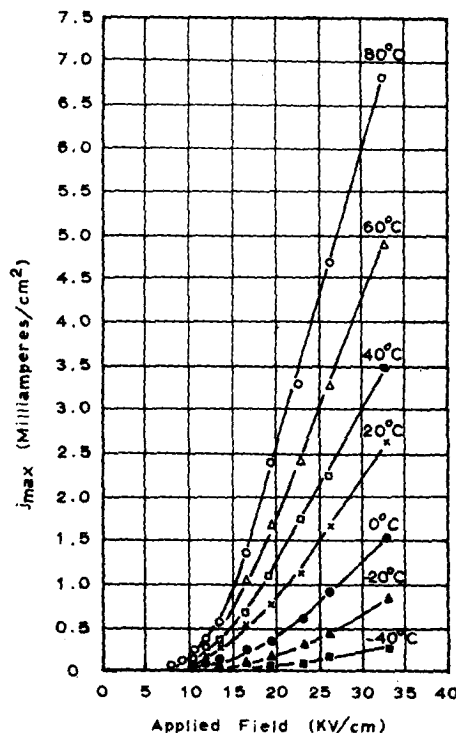


FIG. 4. Fused  $\text{KNO}_3$  peak switching current density versus applied field at several temperatures (copper substrate; silver paint 2nd electrode).

is noted at high fields, indicating, for switching applications, that the element may be approximated by a resistance in series with a voltage bias. These data can be correlated to those of Fig. 3: At higher temperatures the ferroelectric dipoles reverse in a shorter time interval; therefore, it is logical that the peak switching current be larger at higher temperatures.

<sup>1</sup> J. P. Nolte and N. W. Schubring, Phys. Rev. Letters 9, 285 (1962).  
<sup>2</sup> W. J. Merz, Phys. Rev. 95, 690 (1954).

### Differing Results Obtained in the Doping of Semiconductors by Energetic Ions

J. O. McCALDIN AND A. E. WIDMER  
 North American Aviation Science Center,  
 Canoga Park, California  
 (Received 12 December 1963)

CONFLICTING results have been reported on the doping of semiconductors by energetic ions. The purpose of this communication is to call attention to certain experimental parameters which are important in resolving these discrepancies.

In 1955 Cussins<sup>1</sup> bombarded Ge with twelve species of energetic ions, ranging in mass from H to Sb, to produce the same doping effect as occurs in electron bombardment, i.e., a radiation damage effect. This effect was almost completely independent of the species of bombarding ion. On the other hand, a recent account<sup>2</sup> of energetic  $\text{Cs}^+$  bombardment of Si under apparently similar conditions

indicates a doping effect due to the chemical nature of the bombarding ion instead of to a radiation damage effect. These apparently contradictory results are due, we believe, to the target temperature during the bombardment and the influence of this temperature on the removal of damage centers. When the target is bombarded cold, as in Cussins work,<sup>1</sup> damage centers dominate the doping effect almost completely, since the damage ratio, i.e., number of target atoms displaced per incident ion, is significantly larger than unity.<sup>3</sup> At the intermediate target temperatures produced by an intense ion beam, as in the work of Medved *et al.*,<sup>2</sup> a mixture of bombardment-damage and chemical-doping results. We note that the unexplained but large differences between their run No. 1 and run No. 2 are in the proper direction to be understood as beam heating effects. Finally when the target is maintained at sufficiently high temperatures,<sup>4</sup> chemical doping is dominant. Using controlled target temperatures, we have produced the full range<sup>5</sup> of doping effects from damage-dominated to chemical-dominated.

A second point of disagreement arises for the concentration of donor centers produced in alkali ion bombardment. A concentration in the surface layer of  $10^{16} \text{ cm}^{-3}$  has been reported by Medved *et al.*,<sup>2</sup> compared to our previous estimate<sup>4</sup> of  $10^{20} \text{ cm}^{-3}$ . Differences in target temperature, just discussed, may be an influence. However, a more important factor, we believe, is that measurements made on a  $p$ - $n$  junction produced by alkali ion injection cannot be extrapolated to the target surface, at least for the bombardment conditions<sup>2,4</sup> presently under discussion. These conditions produce<sup>6</sup> a heavily doped surface layer in the region where the original ion penetration takes place, and, in addition, a gently graded diffusion "tail" which may extend<sup>7</sup> many microns into the target crystal. The  $p$ - $n$  junction, particularly for a target crystal of high initial resistivity, lies principally in the diffusion tail, as is shown by capacitance measurements<sup>8,9</sup> made on the junction. Therefore, measurements made in the vicinity of the junction; e.g., the estimates of Medved *et al.*<sup>2</sup> for donor concentration, cannot be extrapolated to characterize conditions at the target surface. We conclude that our original figure of  $\sim 10^{20} \text{ cm}^{-3}$  for the donor concentration at and near the target surface, which was based on relatively direct measurements, is still the best estimate.

<sup>1</sup> W. D. Cussins, Proc. Phys. Soc. (London) **B68**, 213 (1955).

<sup>2</sup> D. B. Medved, G. P. Rolik, R. C. Speiser, and H. L. Daley, Appl. Phys. Letters **3**, 213 (1963).

<sup>3</sup> See, for example, J. R. Beeler, Jr., and D. G. Besco, J. Appl. Phys. **34**, 2873 (1963) who calculate a damage ratio of  $\sim 5$  to  $\sim 50$  under conditions comparable to those discussed here; Also see M. M. Bredov, V. A. Lepilin, I. B. Shestakov, and A. L. Shakh-Budagov, Fiz. Tverd. Tela **3**, 267 (1961) [English transl.: Soviet Phys.—Solid State **3**, 195 (1961)].

<sup>4</sup> J. O. McCaldin and A. E. Widmer, J. Phys. Chem. Solids **24**, 1073 (1963).

<sup>5</sup> See, Ref. 4, p. 1077.

<sup>6</sup> J. O. McCaldin and A. E. Widmer, Proc. IEEE (to be published).

<sup>7</sup> J. O. McCaldin, A. L. Widmer, and J. Glass, Bull. Am. Phys. Soc. **9**, (1963) (for Philadelphia A. P. S. meeting) to be published.

<sup>8</sup> J. O. McCaldin and A. E. Widmer, Bull. Am. Phys. Soc. **8**, 473 (1963).

## Production of Particulate Beams

W. K. MURPHY\* AND G. W. SEARST

Research Division, General Dynamics/Electronics, Rochester, New York  
(Received 26 August 1963; in final form 24 February 1964)

IT is the purpose of this note to describe a general method of producing particulate beams, i.e., rectilinearly moving streams of microscopic particles, for use in an evacuated chamber. The particles are produced as an aerosol or smoke, at or near atmospheric pressure, and admitted to the high vacuum chamber through a sequence of individually pumped preliminary chambers that are connected by short lengths of coaxial capillaries. The capillaries offer almost no resistance to particle flow but substantial resistance to the flow of carrier gas. The particulate beam is mainly confined to a very small solid angle about the capillary axis; approximately one out of ten particles entering the first chamber, with velocity nearly that of the carrier gas molecules, is found in the final beam. The production of particulate beams for

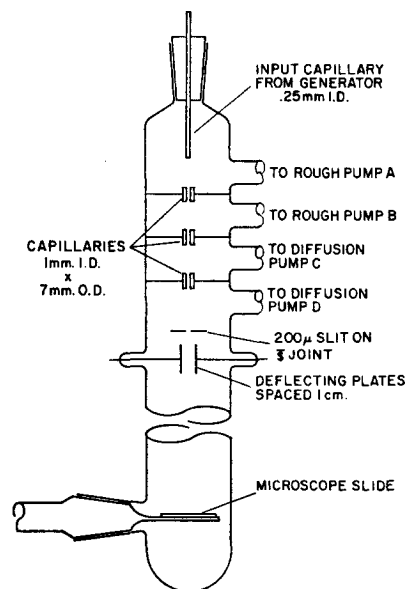


FIG. 1. Schematic diagram of a particulate beam source. The smoke generator (not shown) is above the apparatus as shown; the beam is finally defined by the 200- $\mu$  slit in the highest vacuum region.

use in the ultrahigh vacuum region is a straightforward extension of the techniques described herein.

In our experiments molybdenum oxide smoke ( $\text{MoO}_3$ ) was generated by electrically heating a 0.5-mm-diam molybdenum filament to red heat in air at pressures ranging from 50–300 Torr. The smoke entered chamber A of the apparatus shown diagrammatically in Fig. 1, through a 10-cm length of stainless steel tubing 0.25-mm i.d. and 0.45-mm o.d. The input capillary was coaxial with three successive sections of 1-mm bore Pyrex capillary, 2 cm in length, spaced 4 cm apart. The capillaries led to successive chambers B, C, and D, each evacuated by its own pumping system. A and B were evacuated by mechanical pumps; C and D were evacuated by two-stage mercury vapor pumps. With an input pressure of 100 Torr, a pressure of  $10^{-6}$  Torr was attained in chamber D.

The particulate beam was detected by its deposit upon a microscope slide. In a typical experiment a visible deposit formed in two to three minutes. After a 45-cm flight from the final 1-mm bore capillary, the beam had diverged only slightly to give a deposit  $\sim 8$  mm in diameter. This corresponds to a solid angle of  $2.5 \times 10^{-4}$  sr. This angle is subject to the assumption that the optical density of the deposit is a fair representation of the density of the impinging beam. Under most conditions this appeared to be a valid assumption.

The average velocity of particles in the beam was determined by standard ballistic methods. The beam traveled vertically downwards through a narrow slit and impinged upon a microscope slide. The transverse optical density of the deposit was measured with a recording densitometer. With the slide replaced in its holder, the experimental assembly was rotated  $90^\circ$  and the beam, now horizontal, was deflected downward by gravity. A second deposit was made below the original. In Fig. 2 a photograph of the undeflected deposit, A and the deflected deposit, B is shown. The transverse optical density of the pair of deposits was measured, and the distance between maxima was taken as the beam deflection. The calculated velocities ranged from 1900 to 6000 cm/sec, dependent upon input pressure and length and bore of the input capillary. For a given input pressure and a given capillary the positions of the beam maxima were reproducible to about 10%.

It was found qualitatively that most particle velocities in the beam differed little from the average velocity. The average measured velocities ranged from 20% to 60% of the rms thermal speeds of the carrier molecules. The rms thermal speed of a particle